A variational mode expansion mode solver

O. V. Ivanova, M. Hammer, R. Stoffer, E. van Groesen

MESA+ Institute for Nanotechnology, AAMP group, University of Twente,
P.O. Box 217, 7500 AE, Enschede, The Netherlands

A variational approach for the semivectorial modal analysis of dielectric waveguides with arbitrary piecewise constant rectangular 2D cross-sections is developed. It is based on a representation of a mode profile as a superposition of modes of constituting slab waveguides times some unknown continuous coefficient functions, defined on the entire coordinate axis. The propagation constant and the lateral functions are found from a variational principle. It appears that this method with one or two modes in the expansion preserves the computational efficiency of the standard effective index method while providing more accurate estimates for propagation constants, as well as well-defined continuous approximations for mode profiles. By including a larger number of suitable trial fields, the present approach can also serve as a technique for rigorous semivectorial mode analysis.

1 Introduction

A variety of methods has been developed for the modal analysis of dielectric waveguides. References [1], [2], [3] present a detailed overview of the techniques. Among these, one of the most popular approximate approaches is the Effective Index Method (EIM) [4]. While being rather intuitive and computationally very efficient, the inherent approximations limit the range of its applicability: problems that occur are e.g. undefined effective indices in a slab region below cut-off and, as a result, only rather heuristically defined field profiles. Several methods exist that in certain respects might be viewed as improvements of the EIM; we mention the (Film) Mode Matching Method (MMM) [5] [6], in which the total field is expanded in the terms of the local slab modes and later matched across the interfaces, the Spectral Index Method [7], in which the total field is put to zero at certain distances from the interfaces with strong refractive index contrast and later expanded in Fourier series, the Weighted Index Method [8], which using a variational procedure finds the modal field profile as the best separable solution of the wave equation and finally the Rigorous Effective Index Method [9], which, for rib waveguides with outer slices above cut-off, by variational means finds a simple transcendental equation for the propagation constant.

In this paper we propose a Variational Mode Expansion Method (VMEM), which uses modes of the constituting waveguides in the representation of the field not only in the corresponding slab, but in the whole waveguide. On the basis of these field templates, approximations for guided modes are then derived by consistently applying a variational restriction procedure. A characteristic feature of this method is that by using continuous field templates the mode field profiles that are found are automatically continuous.

On the one hand, if one or two modes are used in the expansion this method can be viewed as an alternative approach for improvement of the EIM, preserving its computational efficiency. On the other hand, by including a large number of suitable basis fields, the present approach can also serve as a technique for rigorous semivectorial mode analysis. In that case the MMM (restricted to scalar / semivectorial calculations) and the present VMEM appear to be quite similar, because both methods are based on expansion into slab modes. Still there are several differences. First, in the MMM the eigenmodes of each slice are used for the representation of the field of only that particular slice, while in VMEM they also contribute to the solution on all other slices. Second, due to the specific field template the VMEM field profiles are automatically continuous (even with only one mode in the expansion), contrary to the MMM solutions. And third, the VMEM is rigorously derived from a variational principle, rather than by employing projection techniques as is commonly seen in the MMM. The variational background of the VMEM leads to certain properties of the solution, e.g. a monotonous convergence of the propagation constants.

The paper is organized as follows. In the next section we put the problem of finding guided modes in a variational form. In section 3 the theory behind the VMEM is outlined. Subsection 3.2 comments on the relation of the present approach with equations familiar from the ”standard” EIM. Results of calculations for a series of waveguide structures including several benchmark examples are given in section 4. Finally, in section 5 conclusions are presented. In view of the fact that the formulation of the VMEM is similar for both TE and TM polarization, the general theory will be provided only for the former, while the equations which differ in the case of TM polarization will be given in the appendix.

2 Variational form of the mode problem

Consider a z-invariant dielectric waveguide given by a piecewise constant refractive index distribution $n(x, y)$ on its cross-section Ω. We are searching for nontrivial solutions of the scalar TE mode equations for the dominant electric field component $E = E_y(x, y)$:

$$\Delta E + k_0^2 n^2(x, y)E = \beta^2 E, \quad (x, y) \in \Omega \tag{1}$$

in the form of profiles, propagating in the z-direction with propagation constant β at given vacuum wavelength $\lambda = 2\pi/k_0$.

There are two cases to be distinguished. On the one hand, if the computational window covers the entire cross section plane $\Omega = \mathbb{R}^2$ a solution of Eq. (1) should be a continuous square integrable function on $\mathbb{R}^2$. On the other hand, for a rigorous analysis, the computational window can be restricted to be bounded in the x-direction, $x \in [x_0, x_1]$, while it remains to be unbounded in the y-direction. In this case the nullity on the boundaries $x = x_0$ and $x = x_1$ of a solution of Eq. (1) is required.

The problem of finding a solution to (1) is equivalent to finding critical points – pairs $\{\beta; E\}$ – of the functional

$$\beta^2 = \mathrm{crit}_{E\in\mathcal{C}(\Omega)}\left\{ \int\limits_{\Omega} \left\{ -|\nabla E|^2 + k_0^2 n^2(x, y)E^2 \right\} dx\, dy \;\Big|\; \int\limits_{\Omega} E^2\, dx\, dy = 1 \right\}. \tag{2}$$

In case Ω is bounded in x-direction the critical points should be searched in the set of functions that vanish on the boundary; this is included as an extra condition.

Using the principle of eigenvalue comparison the variational viewpoint permits a few direct conclusions concerning the influence of the computational window and the sets of trial functions. Namely, let β_s^2 be the highest critical value of the functional (2) over the set of all functions $\mathcal{C}^0(\Omega_s)$, continuous functions defined on the computational domain Ω_s with zero on its boundary. Then by increasing the computational domain $\Omega_b \supset \Omega_s$ and taking the corresponding set $\mathcal{C}^0(\Omega_b) \supset \mathcal{C}^0(\Omega_s)$, the highest critical value β_b^2, found from (2), can only increase: $\beta_b^2 \geq \beta_s^2$. Consequently, with increasing computational domain, the approximation of the propagation constant of the fundamental mode will approach its exact value from below.

Next, let Ω be a fixed domain and let $\beta^2_{\Omega,\mathcal{E}_1}$ and $\beta^2_{\Omega,\mathcal{E}_2}$ be the principal critical values of the functional (2) considered over the sets of the functions $\mathcal{E}_1$ and $\mathcal{E}_2$ correspondingly, defined over domain Ω. If $\mathcal{E}_1 \subset \mathcal{E}_2$, then from the principle of eigenvalue comparison it follows that $\beta^2_{\Omega,\mathcal{E}_1} \leq \beta^2_{\Omega,\mathcal{E}_2}$. In other words, by increasing the number of trial functions on the same domain the approximation value for the propagation constant of the fundamental mode can only increase.

3 Variational mode expansion method

Upon a division of the waveguide cross-section into r y-homogeneous slices $S_1, \ldots, S_r$ with refractive index distribution $n_1(x), \ldots, n_r(x)$, the principal field component $E = E_y(x, y)$ is represented as a superposition of TE modes $X_i(x)$ of the constituting slab waveguides, times some unknown continuous coefficient functions $Y_i(y)$:

$$E(x, y) = \sum_{i=1}^{N} X_i(x)Y_i(y). \tag{3}$$

Fig. 1 shows an example and introduces the Cartesian axes x, y.

Note that functions $Y_i(y)$ are defined on the whole y – axis, which implies that modes $X_i(x)$ are relevant for the field in the whole waveguide. In the section 3.1 we will explain the process of selecting modes $X_i(x)$, while here we describe the method of finding the coefficient functions.

Restricting the functional (2) to the trial field (3) we arrive at the new problem of finding the critical points $\{\beta; Y_1, \ldots, Y_N\}$ of the functional

$$\beta^2 = \mathrm{crit}_{\{Y_1,\ldots,Y_N\}\in\mathcal{C}(\mathbb{R})}\left\{ \int\limits_{\Omega} \Big\{ -\Big|\nabla\big(\sum_{i=1}^{N} X_i(x)Y_i(y)\big)\Big|^2 + k_0^2 n^2(x, y)\big(\sum_{i=1}^{N} X_i(x)Y_i(y)\big)^2 \Big\}\, dx\, dy \;\Big|\right.$$

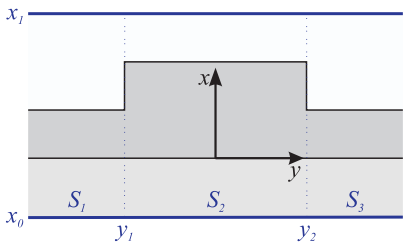

Figure 1: Sample geometry: rib waveguide. In this case the structure can be divided by vertical lines at y_1, y_2 into three slices S_1, S_2, S_3 with homogeneous refractive index destribution along the y - axis. As discussed in section 2, the mode problem will be considered on the entire x - axis, or, alternatively, on a computational window $x \in [x_0, x_1]$.

$$\int_\Omega \Big(\sum_{i=1}^{N} X_i(x) Y_i(y) \Big)^2 \, dx \, dy = 1 \Big\}. \tag{4}$$

Requiring this functional to become stationary leads to a vectorial differential equation, for the unknown function $\mathbf{Y}(y) = (Y_1(y), \ldots, Y_N(y))$ with the propagation constant β as a parameter, of the form

$$\mathbf{F}\mathbf{Y}''(y) + \mathbf{M}(y)\mathbf{Y}(y) = \beta^2 \mathbf{F}\mathbf{Y}(y). \tag{5}$$

The matrices $\mathbf{F}$ and $\mathbf{M}$ are of dimension $N \times N$ and consist of elements

$$F_{g,h} = \int_{x_0}^{x_1} X_g(x) X_h(x) \, dx, \tag{6}$$

$$M_{g,h}(y) = \int_{x_0}^{x_1} \left(k_0^2 n^2(x,y) X_g(x) X_h(x) - X_g'(x) X_h'(x) \right) \, dx. \tag{7}$$

Note that inside each constituting slice the matrix $\mathbf{M}$ does not depend on y, so in the slice S_j we can denote it as $\mathbf{M}^{(j)}$.

Beyond (5), for a structure divided into slices, stationarity of (4) amounts to interface conditions of continuity of

$$\mathbf{Y}(y) \qquad \text{(as an essential condition)} \tag{8}$$

and

$$\mathbf{Y}'(y) \qquad \text{(as a natural condition).} \tag{9}$$

Consequently the profiles $\mathbf{Y}$ now can be found by solving in the each separate slice S_j the vectorial differential equation with constant coefficients:

$$\left(\mathbf{Y}^{(j)}\right)'' + \mathbf{T}^{(j)}\mathbf{Y}^{(j)} = \beta^2 \mathbf{Y}^{(j)}, \quad \text{where } \mathbf{T}^{(j)} = \mathbf{F}^{-1}\mathbf{M}^{(j)} \tag{10}$$

and matching the solutions across the interfaces according to the conditions (8) and (9).

Searching for solutions in the form of $\mathbf{Y}^{(j)} = \exp(\mu^{(j)} y)\mathbf{p}_j$, Eq. (10) requires that in the j-th slice the values $\mu^{(j)}$ and the vectors $\mathbf{p}^{(j)}$ satisfy the eigenvalue problem

$$\mathbf{T}^{(j)}\mathbf{p}^{(j)} = \eta^{(j)}\mathbf{p}^{(j)}, \quad \text{with } \eta^{(j)} = \beta^2 - \left(\mu^{(j)}\right)^2 \tag{11}$$

as eigenvalues and $\mathbf{p}^{(j)}$ as eigenvectors, which do not depend on β. Note that all the $\mu^{(j)}$ do. Since the matrix $\mathbf{T}^{(j)}$ is of dimension $N \times N$, solving the eigenvalue problem (11) yields N eigenvalues $\eta_1^{(j)}, \ldots, \eta_N^{(j)}$ and corresponding eigenvectors $\mathbf{p}_1^{(j)}, \ldots, \mathbf{p}_N^{(j)}$. From the fact that the matrix $\mathbf{F}$ is symmetric positive definite and the matrix $\mathbf{M}^{(j)}$ is symmetric we can conclude that the matrix $\mathbf{T}^{(j)} = \mathbf{F}^{-1}\mathbf{M}^{(j)}$ has only real eigenvalues. Looking only for exponentially decaying functions towards $\pm\infty$, the solution of (10) will be

$$\mathbf{Y} = \begin{cases} \mathbf{Y}^{(j)} = \sum\limits_{i=1}^{N} \left(a_i^{(j)} \exp(\mu_i^{(j)} y) + b_i^{(j)} \exp(-\mu_i^{(j)} y)\right) \mathbf{p}_i^{(j)}, \quad j = 2, \ldots, r-1 \quad \text{(in the each inner slice)}; \\ \mathbf{Y}^{(1)} = \sum\limits_{i=1}^{N} d_i \exp(\mu_i^{(1)} y) \mathbf{p}_i^{(1)} \quad \text{(in the left outer slice)}; \\ \mathbf{Y}^{(r)} = \sum\limits_{i=1}^{N} c_i \exp(-\mu_i^{(r)} y) \mathbf{p}_i^{(r)} \quad \text{(in the right outer slice)}, \end{cases}$$

where all $\mu_i^{(1)}$ and $\mu_i^{(r)}$ must be positive, while in the inner slices the $\mu_i^{(j)}$ can be complex conjugate pairs. To ensure the former, β must be larger than the square root of the highest eigenvalue among $\eta_1^{(1)}, \ldots, \eta_N^{(1)}$ and $\eta_1^{(r)}, \ldots, \eta_N^{(r)}$, as it follows from (11). Moreover, to satisfy the continuity requirements (8), (9) across the interfaces, at least in one of the inner slices $\mathbf{Y}^{(j)}$ must have harmonic behavior, which implies that β must be smaller than the square root of the highest eigenvalue among those which corresponds to the inner slices: $\eta_1^{(j)}, \ldots, \eta_N^{(j)}$. Thus an interval $\mathcal{I}_\beta$ for admissible values β is found.

Still the coefficients $\mathbf{a}^{(j)}, \mathbf{b}^{(j)}, \mathbf{c}$ and $\mathbf{d}$ have to be determined (where to shorten the notation we put $\mathbf{a} = [a_1, \ldots, a_N]$ etc). If the interface between slice S_j and S_{j+1} is $y = y^{(j)}$, by using the interface conditions (8) and (9) the following system of equations arises:

$$\mathbf{Y}^{(j)}(y^{(j)}) = \mathbf{Y}^{(j+1)}(y^{(j)}), \tag{12}$$

$$\left(\mathbf{Y}^{(j)}(y^{(j)})\right)' = \left(\mathbf{Y}^{(j+1)}(y^{(j)})\right)', \quad j = 1, \ldots, r-1, \tag{13}$$

or, in matrix form,

$$\mathbf{V}\mathbf{f} = 0, \tag{14}$$

with a vector of all unknown coefficients,

$$\mathbf{f} = [\mathbf{d},\ \mathbf{a}^{(2)},\ \mathbf{b}^{(2)},\ \ldots,\ \mathbf{a}^{(r-1)},\ \mathbf{b}^{(r-1)},\ \mathbf{c}]^\intercal,$$

and the matrix

$$\mathbf{V} = \begin{bmatrix} \mathbf{V}^d & \mathbf{V}_{2-}^{ab} & & & & \\ & \mathbf{V}_{2+}^{ab} & \mathbf{V}_{3-}^{ab} & & \mathbf{0} & \\ & & \ddots & & & \\ & \mathbf{0} & & \mathbf{V}_{(r-2)+}^{ab} & \mathbf{V}_{(r-1)-}^{ab} & \\ & & & & \mathbf{V}_{(r-1)+}^{ab} & \mathbf{V}^c \end{bmatrix},$$

whose s-th line represents all the continuity conditions at the s-th interface. The columns of the submatrices can be written as:

$$\mathbf{V}^d(i) = \begin{bmatrix} \exp(\mu_i^{(1)} y^{(1)}) \mathbf{p}_i^{(1)} \\ \mu_i^{(1)} \exp(\mu_i^{(1)} y^{(1)}) \mathbf{p}_i^{(1)} \end{bmatrix}, \qquad \mathbf{V}^c(i) = \begin{bmatrix} -\exp(-\mu_i^{(r)} y^{(r-1)}) \mathbf{p}_i^{(r)} \\ \mu_i^{(r)} \exp(-\mu_i^{(r)} y^{(r-1)}) \mathbf{p}_i^{(r)} \end{bmatrix}, \tag{15}$$

$$\mathbf{V}_{j-}^{ab} = \begin{bmatrix} \mathbf{A}_{j-} & \mathbf{B}_{j-} \end{bmatrix}, \qquad \mathbf{V}_{j+}^{ab} = \begin{bmatrix} \mathbf{A}_{j+} & \mathbf{B}_{j+} \end{bmatrix},$$

where

$$\mathbf{A}_{j-}(i) = \begin{bmatrix} -\exp(\mu_i^{(j)} y^{(j-1)}) \mathbf{p}_i^{(j)} \\ -\mu_i^{(j)} \exp(\mu_i^{(j)} y^{(j-1)}) \mathbf{p}_i^{(j)} \end{bmatrix}, \qquad \mathbf{B}_{j-}(i) = \begin{bmatrix} -\exp(-\mu_i^{(j)} y^{(j-1)}) \mathbf{p}_i^{(j)} \\ \mu_i^{(j)} \exp(-\mu_i^{(j)} y^{(j-1)}) \mathbf{p}_i^{(j)} \end{bmatrix}, \tag{16}$$

$$\mathbf{A}_{j+}(i) = \begin{bmatrix} \exp(\mu_i^{(j)} y^{(j)}) \mathbf{p}_i^{(j)} \\ \mu_i^{(j)} \exp(\mu_i^{(j)} y^{(j)}) \mathbf{p}_i^{(j)} \end{bmatrix}, \qquad \mathbf{B}_{j+}(i) = \begin{bmatrix} \exp(-\mu_i^{(j)} y^{(j)}) \mathbf{p}_i^{(j)} \\ -\mu_i^{(j)} \exp(-\mu_i^{(j)} y^{(j)}) \mathbf{p}_i^{(j)} \end{bmatrix} \tag{17}$$

for $i = 1, \ldots, N,\ j = 1, \ldots, r-1$. Propagation constants β are thus those values from the interval $\mathcal{I}_\beta$ for which a nontrivial solution of Eq. (14) exists, i.e. those for which at least one eigenvalue of $\mathbf{V}$ becomes zero. Corresponding field profies $E(x, y)$ can be found from Eq. (3).

3.1 Modal basis functions

Let the refractive index destribution in the waveguide within the j-th slice be $n_j(x)$. The corresponding modes are continuous solutions with continuous derivatives of

$$X''(x) + k_0^2 n_j^2(x) X(x) = \gamma^2 X(x), \tag{18}$$

with γ as a propagation constant. There are two cases to be distinguished:

- If the computational window is unbounded, solutions of (18) must be square integrable. There is only a finite number of them.
- If the computational window in x - direction is $x \in [x_0, x_1]$, solutions of (18) are chosen to be zero at the boundary. There are infinitely many of them and, moreover, they form a complete discrete set of functions defined on $[x_0, x_1]$ with zero Dirichlet boundary conditions.

The detailed process of finding the solutions of Eq. (18) can be found e.g. in [10]. Ensuring positive-definiteness of the matrix $\mathbf{F}$ requires linear independence of the trial functions. This means that one should select which modes X to take into expansion (3). Obviously a safe choice is to take a finite set of modes from a single slice. At the same time when taking into the expansion only a few modes, it is sometimes possible and, as our results show, beneficial to take also into account modes from other slices.

3.2 Relation with EIM

While the equations in Section 3 appear rather involved, it is instructive to write them out for a case in which there is only one slab mode in the expansion. By taking only one term $E = X(x)Y(y)$ in the expansion (3) (with X a mode profile of a reference slice; for the rib of Fig. 3 this would typically be the guided mode of the inner slice), according to (5) the corresponding equation for the function Y is

$$Y''(y) + \frac{\int_{x_0}^{x_1} \left(k_0^2 n^2(x,y) X^2(x) - (X'(x))^2\right) dx}{\int_{x_0}^{x_1} X^2(x)\, dx} Y(y) = \beta^2 Y(y). \tag{19}$$

As a slab waveguide mode profile, X satisfies the equation

$$X''(x) + k_0^2 n_r^2(x) X(x) = \gamma^2 X(x) \tag{20}$$

for propagation constant γ, where n_r is the refractive index profile of the reference slice. By inserting this equation into (19) and integrating by parts, we obtain, after defining the effective index N_{eff} of the mode profile X of the slice r through $\gamma = k_0 N_{\text{eff}}$:

$$Y''(y) + k_0^2 \left(N_{\text{eff}}^2 + \frac{\int_{x_0}^{x_1} \left(n^2(x,y) - n_r^2(x)\right) X^2(x)\, dx}{\int_{x_0}^{x_1} X^2(x)\, dx} \right) Y(y) = \beta^2 Y(y). \tag{21}$$

Hence the equation for the lateral profile function Y as it emerges from the variational procedure is similar to what is used in the EIM: in the reference slice one has $n(x,y) = n_r(x)$, and the effective index appears to be the one corresponding to the mode profile X; in other slices this effective index is modified by the difference between the local permittivity and that of the reference slice, weighted by the local intensity of the reference mode profile. This means that even in slices in which there is no local mode above cut-off, a reasonable "effective index" can still be defined. Note that this recipe results directly from the application of the variational procedure; no heuristics are needed beyond the ansatz (3).

4 Numerical results and comparisons

In short, the whole numerical procedure of mode finding can be outlined as follows: find the set of basis modes X_i; calculate matrices $\mathbf{T}_j$ and their eigenvectors and eigenvalues according to Eq. (11); determine the interval $\mathcal{I}_\beta$ for admissible values of β; identify values of β from this interval, for which the matrix $\mathbf{V}$ from (14) has at least one zero eigenvalue; for each found propagation constant β assemble the corresponding field profile according to Eq. (3). The validity of the method was checked for several waveguide structures. It should be mentioned that in all of the following examples our results agree remarkably well with rigorous numerical finite-element FEMLAB [11] solutions of the Eqs. (1) or (A-1).

4.1 Rib waveguide

A frequently investigated geometry for comparison of mode analysis methods [2], [15] is shown in Fig. 2(a). The structure can be divided into three slices S_1, S_2, S_3. Inside these slices the refractive index distribution is homogeneous along the y - axis. Since the first and last slices are equal, we will take into expansion (3) only modes from the first and second slices.

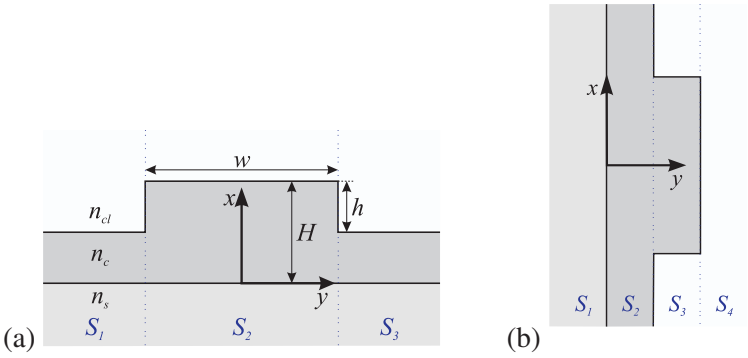

Figure 2: Cross section of a benchmark rib waveguide. Geometrical parameters: $w = 3\mu m$, varying h, $H = 1\mu m$, refractive indices: $n_s = 3.4$, $n_c = 3.44$, $n_{cl} = 1.0$, operating wavelength $\lambda = 1.15\mu m$. (a) "Conventional" division into slices, computational window $x \in [-10, 10]\mu m$; (b) an alternative division of the rotated structure.

In Fig. 3 propagation constants of the fundamental TE and TM modes, obtained by other methods, are compared to those of the VMEM. As was discussed in section 2, with enlarging the mode set the propagation constant β increases and thus approaches its exact value from below. Note that very accurate results compared to the rigorous finite element (FEMLAB) solutions can be obtained using only 16 modes in the expansion (3).

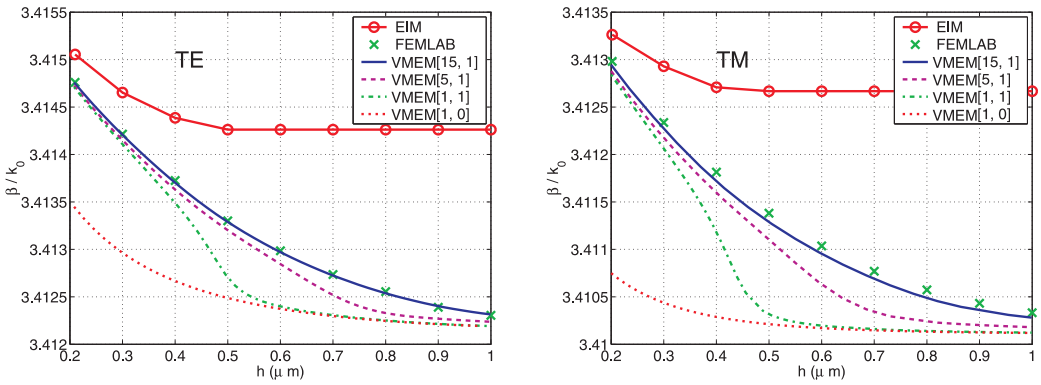

Figure 3: Effective indices (β/k_0) of the fundamental TE and TM modes supported by the waveguide of Fig. 2(a) as a function of the rib height h. EIM: effective index method; FEMLAB: finite element [11] calculations on a mesh with about 20,000 elements and a computational window $(x, y) \in [-6.5, 2.5] \times [-7.5, 7.5]$; VMEM [i,j]: the present method with i and j modes of slices S_2 and S_1 correspondingly, used in the expansion (3).

In Fig. 4 we show X, Y and total field profiles of the fundamental TE modes for the VMEM[1,0], VMEM[1,1] and VMEM[5,1], for $h = 0.4\mu m$. From the Y profiles one can see that in this structure the field in the middle of the inner slice is dominated by the fundamental mode of the inner slice, while in the outer slices the field is dominated by the fundamental mode of the outer slice. Around the interfaces between slices all considered modes play a significant role; apparently they are all needed to satisfy the interface conditions. From Fig. 3 and 4 it follows, that including the outer slice mode significantly improves the estimations of the field profiles as well as propagation constants, while the higher order modes of the inner slice mainly seem to smoothen the field around the interfaces.

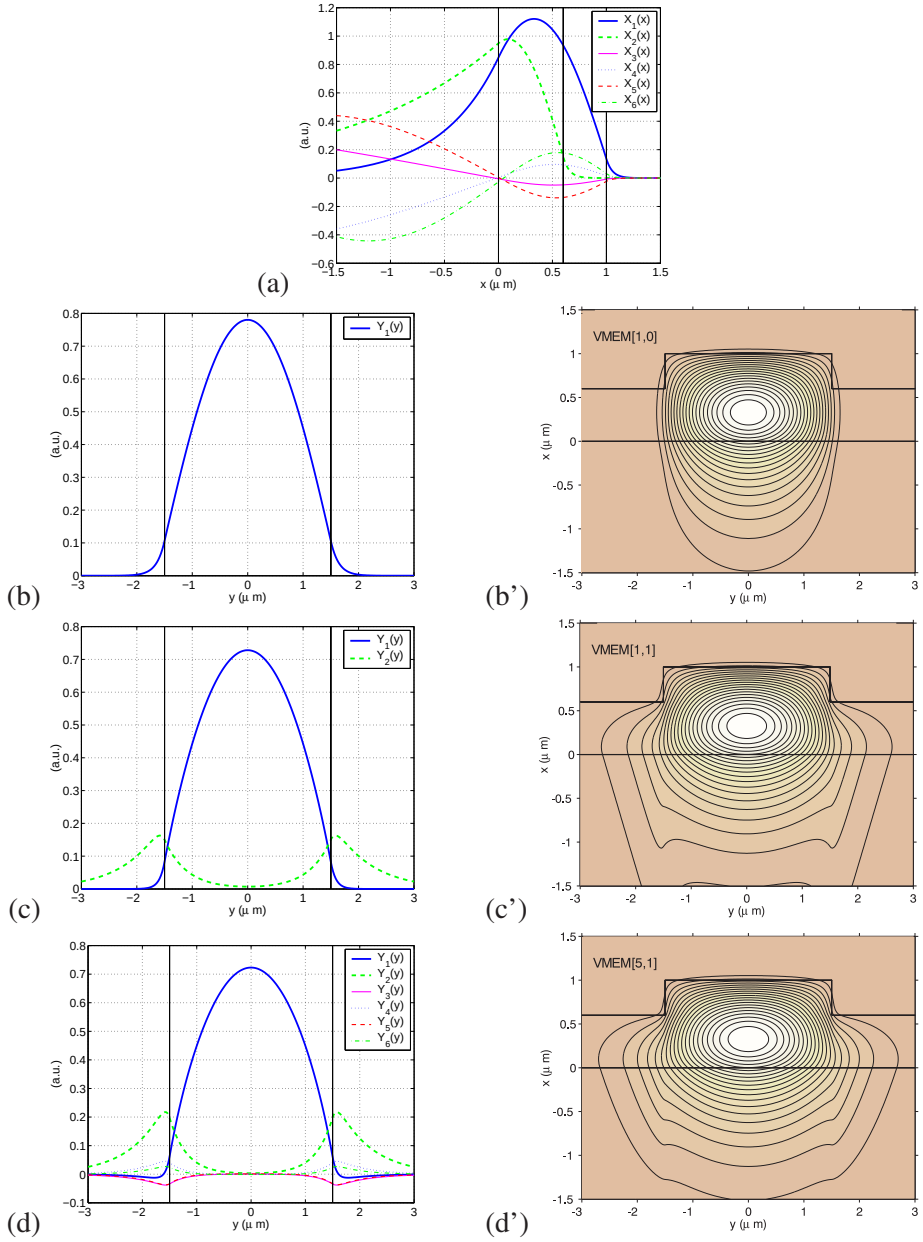

Figure 4: For the rib waveguide structure of Fig. 2(a) with $h = 0.4\mu m$: Plot (a) shows the TE mode profiles X of the constituting slab waveguides: X_1 is the fundamental mode of the inner slice S_2; X_2 is the fundamental mode of the outer slice S_1; X_3, X_4, X_5 and X_6 – first, second, third and fourth order modes of the inner slice S_2 corrspondingly. Plots (b), (c) and (d) show Y profiles and plots (b'), (c') and (d') corresponding field profiles of the fundamental TE mode. (b) and (b') correspond to VMEM[1,0], (c) and (c') to VMEM[1,1], and (d) and (d') to VMEM[5,1].

A division into horizontal layers can be an alternative to the division of the waveguide cross-section described above, as is shown in the Fig. 2(b). There are four layers S_1, S_2, S_3, S_4 with homogeneous refractive index destribution along the y - axis. Effectively modes only from two layers S_3 and S_4 (alternatively, S_1 or S_2) are required.

In Fig. 5 convergence of the effective index of the fundamental TE mode is shown. Note that for the symmetric structure only symmetric modes X of slices S_3 and S_4 have an impact on the field distribution of the symmetric

mode of the whole structure, while antisymmetric will have none – and the other way around for antisymmetric modes. Therefore only even modes are used in Fig. 5.

Already with a moderate number of $15+5$ basis fields a satisfactory convergence in refractive index is achieved, contrary to the results of the Complex General Fourier Variational Method in [12] where many more basis modes are needed.

While according to the figure the effective index β/k_0 obtained on a larger computational window L is always smaller than the effective index computed with a smaller window for the same number of (different) modes N, this is not the case when high number of terms are taken into account in expansion (3) (the curves cross). As was discussed in section 2, when using the full modal basis sets with increasing computational window the effective index (propagation constant) of the fundamental mode can only increase.

As discussed in Section 3.2, when taking only one mode into the expansion (VMEM[1,0]) the resulting equations are still always well-defined. Contrary to the effective index method, the VMEM produces reasonable results after the outer slice has gone below cut-off, at very similar computational cost.

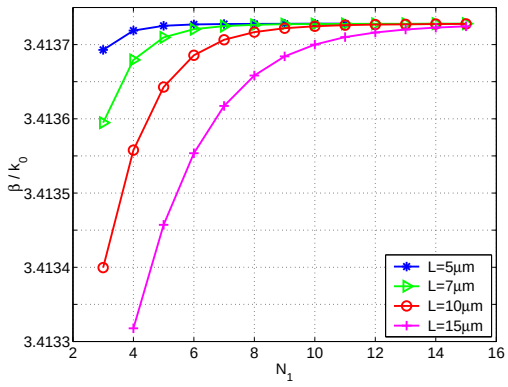

Figure 5: Convergence of the effective index (β/k_0) of the fundamental TE mode for the rib waveguide of Fig. 2(b) ($h = 0.4\mu m$) as a function of the number of even modes from region S_3, used in the expansion (3), for different sizes of the computational window $x \in [-L, L]$. The number of even modes from the region S_4 (equivalently, S_1 or S_2), used in the expansion (3), is always 5.

4.2 Four evanescently coupled ribs

For the analysis of coupler structures, a basic issue is the accurate determination of all "supermode" propagation constants, i.e. fundamental as well as higher order modes are relevant. While finite difference and finite element methods can produce rather accurate results, they require large mesh sizes to cover the waveguide cross-section. The VMEM proves to be applicable for this type of structures.

Fig. 6 introduces a waveguide geometry with four parallel ribs [13]. It can be divided into 9 slices $S_1, \ldots, S_9$ with horizontally homogeneous refractive index destributions. In the field expansion we will take into account modes from two slices, S_2 (alternatively, any other even numbered slice) and S_3 (alternatively, any other odd numbered slice). Table 1 compares normalized propagation constants with results from other methods. Note that even with only quite few modes X_i in the expansion (3) reasonable accuracy in comparison with FEMLAB results can be achieved. The deviation in propagation constants from results of other methods can be due to polarization effects, i.e. due to different approximate mode equations. In Fig. 7 corresponding field profiles are shown.

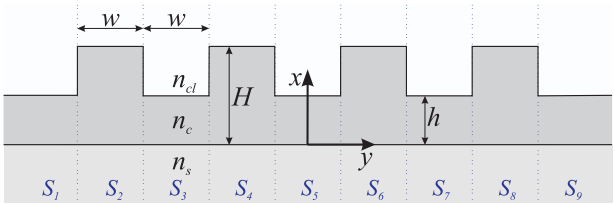

Figure 6: Geometrical parameters of the four rib waveguide structure: $w = 4\mu m$, $H = 6\mu m$, $h = 3\mu m$, refractive indices: $n_s = 3.34$, $n_c = 3.44$, $n_{cl} = 1.0$, operating wavelength $\lambda = 1.55\mu m$. A computational window $x \in [-10, 10]\mu m$ has been used.

b	TE0	TE1	TE2	TE3	TM0	TM1	TM2	TM3
DSI	0.944760	0.943999	0.942957	0.942008	0.944509	0.943852	0.942975	0.942195
EIM	0.959920	0.959118	0.958025	0.957040	0.958671	0.957919	0.956907	0.956006
FEMLAB	0.946091	0.945366	0.944381	0.943493	0.943087	0.942395	0.941462	0.940628
VMEM[3,2]	0.945826	0.945099	0.944104	0.943199	0.942558	0.941863	0.940917	0.940062
VMEM[30,2]	0.946113	0.945392	0.944407	0.943513	0.943019	0.942314	0.941381	0.940539

Table 1. Normalized effective indices $b = ((\beta/k_0)^2 - n_s^2)/(n_c^2 - n_s^2)$ of the four rib waveguide of Fig. 6. DSI: discrete-spectral-index method by Ng et. al. [13], EIM: effective index method, FEMLAB: finite element calculation on a dense mesh and a computational window $(x, y) \in [-10, 10] \times [-20, 20]\mu m^2$, VMEM[i,j]: the present method, where a computational window $x \in [-10, 10]\mu m$ and i and j modes of the slices S_2 and S_3 correspondingly were used in the expansion (3).

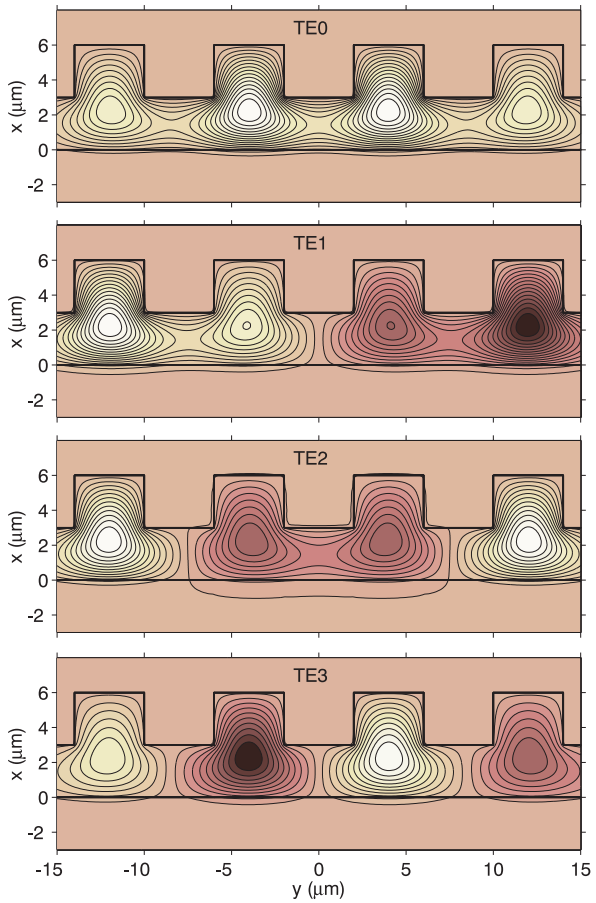

Figure 7: VMEM[30, 2] field profiles of the four rib waveguide of the Fig. 3 for the propagation constants of Table 1.

4.3 3D coupler

Fig. 8 shows the geometry of a three dimensional four waveguide coupler [14], [15]. This waveguide can be divided into five slices with homogeneous refractive index destribution along the y - direction. We performed two calculations: one on an infinite and one on a finite computational window. In the former case only two – one symmetric and one antisymmetric – guided modes exist in the slice S_2 (alternatively, S_4) and none in the slice S_3 (alternativly, S_1 or S_5). It is obvious, that only symmetric modes of constituting slices will influence the estimation of propagation constants and field profiles of symmetric, with respect to y - axis, modes of the whole waveguide, while antisymmetric modes will be irrelevant, and vice versa. If a computational window $x \in [x_0, x_1]$ is used, complete sets of modes exist in all five slices. The reasoning of choosing either symmetric or antisymmetric modes remains valid.

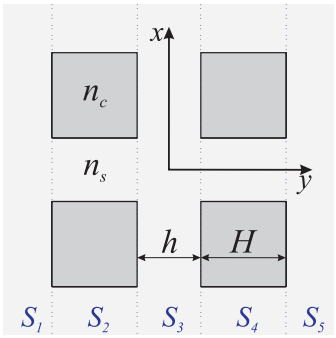

Figure 8: A 3D waveguide coupler – four equidistant square cores of higher refractive index imbedded in a substrate of lower refractive index [14]. Parameteres are $h = 3\mu m$, $H = 4\mu m$, $n_s = 1.506$, $n_c = 1.512$, operating wavelength $\lambda = 1.32\mu m$.

Table 2 compares effective indices, obtained by various other methods and the present one. To calculate propagation constants of modes TE00 and TE01 (TE10 and TE11) only symmetric (antisymmetric) modes were used. Rather accurate estimations of effective indices are achieved already with only one mode in the expansion. Fig. 9 shows the corresponding field profiles.

Due to the fact that slices S_1, S_3, S_5 do not support any guided modes effective indices of these slices are not defined and thus the "standard" EIM cannot be consistently applied to this waveguide geometry. As an approximation to these indices the substrate refractive index n_s was used to compute the EIM effective indices of Table 2. Note that EIM profiles are always discontinuous across the interfaces, while the VMEM fields are well defined and continuous even with one mode in the expansion (3).

	N_{eff}^{00}	N_{eff}^{01}	N_{eff}^{10}	N_{eff}^{11}
VFEM	1.5075807	1.5067966	1.5067966	1.5060260
WMM	1.5078966	1.5071085	1.5071092	1.5064697
EIM	1.5080433	1.5072134	1.5075570	1.5067277
VMEM*[1,0]	1.5077912	1.5069894	1.5069690	1.5061836
VMEM[15,2]	1.5078853	1.5070795	1.5070793	1.5062961

Table 2. Effective indices $N_{\text{eff}} = \beta/k_0$ of the TE modes of the 3D coupler; VFEM: vectorial FEM [14], WMM: wave matching method [15], EIM: effective index method, VMEM[i,j]: the present method with i and j modes of slices S_2 and S_3 correspondingly, used in the field expansion. For the results VMEM* an infinite computational window was used and for VMEM the computational window was $x \in [-20, 20]\mu m$.

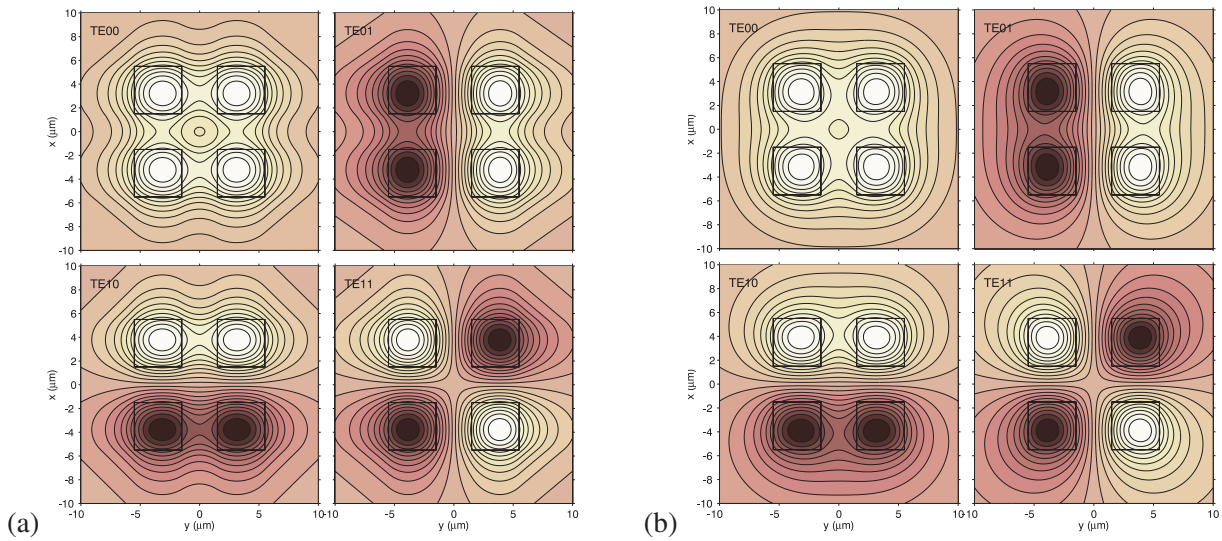

Figure 9: (a) VMEM*[1,0] and (b) VMEM[15,2] field profiles of the 3D coupler.

5 Concluding remarks

A variational method for mode analysis of dielectric waveguides was developed. VMEM results were compared with several other methods on different waveguide geometries. Somewhat remarkably, the comparison indicates that a reasonable accuracy in the computation of propagation constants can be achieved with rather few (sometimes: single) modes in the field expansion. No problem arises, if one of the constituting slices is below cut-off.

It was shown that the VMEM is applicable to waveguides with arbitrary, piecewise constant rectangular cross-section. In principle, also waveguides with arbitrary refractive index distributions (graded index, non-rectangular discontinuities) can be considered, provided these can reasonably be approximated in a staircase manner by slices with piecewise constant rectangular refractive index distribution [16].

Although in this paper we concentrated on scalar / semivectorial analysis, it is expected to be possible to extend this method to vectorial calculations by using the stationary formula for the vectorial mode equations [10] together with suitable templates for the vectorial fields.

6 Acknowledgement

This work is financially supported by NanoNed, flagship NanoPhotonics, project TOE. 7143.

References

[1] K. S. Chiang, "Review of numerical and approximate methods for the modal analysis of general optical dielectric waveguides", *Opt. Quantum Electron.*, **16** (1994).

[2] C. Vassallo, "Mode solvers, 1993 - 1995 optical mode solvers", *Opt. Quantum Electron.*, **29** (1997).

[3] R. Scarmozzino, A. Gopinath, R. Pregla, S. Helfert, "Numerical techniques for modelling guided wave photonic devices", *Journal of selected topics in quantum electronics*, Vol. 6, No. 1 (2000).

[4] R. März, *Integrated optics – design and modelling*, Artech house, Boston, London (1994).

[5] S. T. Peng, A. A. Oliner, "Guidance and leakage properties of a class of open dielectric waveguides. I. Mathematical formulations", *IEEE Trans. Microwave Theory Tech.*, MTT-29 (1981).

[6] A. S. Sudbø, "Film mode matching: a versatile numerical method for vector mode field calculation in dielectric waveguides", *Pure Appl. Opt.*, vol. 2, pp. 211-233 (1993).

[7] C. Vassallo, Y. H. Wang, "A new semirigorous analysis of rib waveguides", *J. Lightwave Technol.*, **8** (1990).

[8] M. J. Robertson, P. C. Kendall, S. Ritchie, P. McIlroy, M. J. Adams, "The weighted index method: a new technique for analysing planar optical waveguides", *J . Lightwave Technol.*, Vol. 8, No. 1 (1990).

[9] T. M. Benson, R. J. Bozeat, P. C. Kendall, "Rigorous effective index method for semiconductor rib waveguides", *IEE Proc. J.*, Vol. 139 (1992).

[10] C. Vassallo, *Optical waveguide concepts*, Elsevier, Amsterdam, 1991.

[11] FEMLAB: http://www.femlab.com.

[12] M. Noureddine, T. M. Benson, C. J. Smartt, P. C. Kendall, "Complex general Fourier variational method applied to the analysis of semiconductor lasers", *IEE Proc.-Optoelectron.*, Vol. 144, No. 4 (1997).

[13] W.-C. Ng, M. S. Stern, "Analysis of multiple-rib waveguide structures by the discrete-spectral-index method", *IEE Proc.-Optoelectron.*, Vol. 145, No. 6 (1998).

[14] L. Friedrich, P. Dannberg, C. Vächter, Th. Hennig, A.Bräuer, W. Karthe, "Directional coupler device using a three-dimentional waveguide structure", *Optics Communications*, 137 (1997).

[15] M. Lohmeyer, PhD Thesis "Guided waves in rectangular integrated magnetooptic devices", Univ. Osnabrück (1999).

[16] K. van de Velde, H. Thienpont, R. van Geen, "Extending the effecive index method for arbitrary shaped inhomogeneous optical waveguides", *Journal of Lightwave technology*, Vol. 6, No. 6 (1988).

7 Appendix

If TM polarized modes are considered, some of the equations in sections 2 and 3 have to be modified as follows. The principal magnetic field component $H = H_y(x, y)$ is to satisfy the scalar TM mode equation

$$\nabla\left(\frac{1}{n^2(x,y)}\nabla H\right) + k^2 H = \beta^2 \frac{1}{n^2(x,y)} H. \tag{A-1}$$

Propagation constants are found as critical points of the variational problem

$$\beta^2 = \mathrm{crit}_{H\in\mathcal{C}(\Omega)}\left\{ \int\limits_{\Omega} \Big\{ -\frac{1}{n^2(x,y)}|\nabla H|^2 + k^2 H^2 \Big\}\, dx\, dy \;\Big|\; \int\limits_{\Omega} \frac{1}{n^2(x,y)} H^2\, dx\, dy = 1 \right\}. \tag{A-2}$$

When restricted to the field template (3) with TM modes, (A-2) reads

$$\beta^2 = \mathrm{crit}_{\{Y_1,\dots,Y_N\}\in\mathcal{C}(\mathbb{R})}\left\{ \int\limits_{\Omega} \Big\{ -\frac{1}{n^2(x,y)}\big|\nabla\big(\sum_{i=1}^{N} X_i(x)Y_i(y)\big)\big|^2 + k^2\big(\sum_{i=1}^{N} X_i(x)Y_i(y)\big)^2 \Big\}\, dx\, dy \;\Big|\right.$$

$$\left. \int\limits_{\Omega} \frac{1}{n^2(x,y)}\big(\sum_{i=1}^{N} X_i(x)Y_i(y)\big)^2\, dx\, dy = 1 \right\}. \tag{A-4}$$

Evaluation of the condition for stationarity leads to the equation

$$\big(\boldsymbol{F}(y)\boldsymbol{Y}'\big)' + \boldsymbol{M}(y)\boldsymbol{Y} = \beta^2 \boldsymbol{F}(y)\boldsymbol{Y} \tag{A-5}$$

with $\boldsymbol{Y}$ and $\boldsymbol{F}(y)\boldsymbol{Y}'$ required to be continuous across the slice interfaces, where the entries of the matrices $\boldsymbol{F}$ and $\boldsymbol{M}$ are

$$\boldsymbol{F}_{g,h} = \int\limits_{x_0}^{x_1} \frac{1}{n^2(x,y)} X_g(x) X_h(x)\, dx, \tag{A-8}$$

$$\boldsymbol{M}_{g,h} = \int\limits_{x_0}^{x_1} \left(k^2 X_g X_h - \frac{1}{n^2(x,y)} X_g' X_h' \right) dx. \tag{A-9}$$

The function $\boldsymbol{Y}$ in each separate slice satisfies the vectorial differential equation with constant coefficients

$$\big(\mathbf{Y}^{(j)}\big)'' + \mathbf{T}^{(j)}\mathbf{Y}^{(j)} = \beta^2 \mathbf{Y}^{(j)}, \quad \text{where } \mathbf{T}^{(j)} = \big(\mathbf{F}^{(j)}\big)^{-1}\mathbf{M}^{(j)}, \tag{A-11}$$

and the continuity conditions are (12) and

$$\mathbf{F}^{(j)}\big(\mathbf{Y}^{(j)}(y^{(j)})\big)' = \mathbf{F}^{(j+1)}\big(\mathbf{Y}^{(j+1)}(y^{(j)})\big)', \quad j = 1, \ldots, r-1. \tag{A-13}$$

Using the exponential form $\exp(\mu^{(j)}y)\mathbf{p}_j$ for $\mathbf{Y}^{(j)}$ within the slice S_j one obtains a system of equations in the form of (14), where the columns of the submatrices are given by

$$\mathbf{V}^d(i) = \begin{bmatrix} \exp(\mu_i^{(1)}y^{(1)})\mathbf{p}_i^{(1)} \\ \mu_i^{(1)}\exp(\mu_i^{(1)}y^{(1)})\mathbf{F}^{(1)}\mathbf{p}_i^{(1)} \end{bmatrix}, \qquad \mathbf{V}^c(i) = \begin{bmatrix} -\exp(-\mu_i^{(r)}y^{(r-1)})\mathbf{p}_i^{(r)} \\ \mu_i^{(r)}\exp(-\mu_i^{(r)}y^{(r-1)})\mathbf{F}^{(r)}\mathbf{p}_i^{(r)} \end{bmatrix}, \tag{A-15}$$

$$\mathbf{A}_{j-}(i) = \begin{bmatrix} -\exp(\mu_i^{(j)}y^{(j-1)})\mathbf{p}_i^{(j)} \\ -\mu_i^{(j)}\exp(\mu_i^{(j)}y^{(j-1)})\mathbf{F}^{(j)}\mathbf{p}_i^{(j)} \end{bmatrix}, \qquad \mathbf{B}_{j-}(i) = \begin{bmatrix} -\exp(-\mu_i^{(j)}y^{(j-1)})\mathbf{p}_i^{(j)} \\ \mu_i^{(j)}\exp(-\mu_i^{(j)}y^{(j-1)})\mathbf{F}^{(j)}\mathbf{p}_i^{(j)} \end{bmatrix}, \tag{A-16}$$

$$\mathbf{A}_{j+}(i) = \begin{bmatrix} \exp(\mu_i^{(j)}y^{(j)})\mathbf{p}_i^{(j)} \\ \mu_i^{(j)}\exp(\mu_i^{(j)}y^{(j)})\mathbf{F}^{(j)}\mathbf{p}_i^{(j)} \end{bmatrix}, \qquad \mathbf{B}_{j+}(i) = \begin{bmatrix} \exp(-\mu_i^{(j)}y^{(j)})\mathbf{p}_i^{(j)} \\ -\mu_i^{(j)}\exp(-\mu_i^{(j)}y^{(j)})\mathbf{F}^{(j)}\mathbf{p}_i^{(j)} \end{bmatrix}. \tag{A-17}$$